INTERNATIONAL ENDODONTIC JOURNAL

doi:10.1111/iej.12628

Micro-CT evaluation of several glide path techniques and ProTaper Next shaping outcomes in maxillary first molar curved canals

M. Alovisi[1], A. Cemenasco[2], L. Mancini[3], D. Paolino[4], N. Scotti[1], C. C. Bianchi[2] & D. Pasqualini[1]

[1]Department of Surgical Sciences, Dental School, Endodontics, University of Turin, Turin; [2]Department of Radiodiagnostics University of Turin, Turin; [3]Elettra Sincrotrone Trieste S.C.p.A Trieste; and [4]Department of Mechanical Engineering and Aerospace Politecnico di Torino, Turin, Italy

Abstract

Alovisi M, Cemenasco A, Mancini L, Paolino D, Scotti N, Bianchi CC, Pasqualini D. Micro-CT evaluation of several glide path techniques and ProTaper Next shaping outcomes in maxillary first molar curved canals. *International Endodontic Journal*.

Aim To evaluate the ability of ProGlider instruments, PathFiles and K-files to maintain canal anatomy during glide path preparation using X-ray computed micro-tomography (micro-CT).

Methodology Forty-five extracted maxillary first permanent molars were selected. Mesio-buccal canals were randomly assigned ($n = 15$) to manual K-file, PathFile or ProGlider groups for glide path preparation. Irrigation was achieved with 5% NaOCl and 10% EDTA. After glide path preparation, each canal was shaped with ProTaper Next X1 and X2 to working length. Specimens were scanned (isotropic voxel size 9.1 μm) for matching volumes and surface areas and post-treatment analyses. Canal volume, surface area, centroid shift, canal geometry variation through ratio of diameter ratios and ratio of cross-sectional areas were assessed in the apical and coronal levels and at the point of maximum canal curvature. One-way factorial ANOVAs were used to evaluate the significance of instrument in the various canal regions.

Results Post-glide path analysis revealed that instrument factor was significant at the apical level for both the ratio of diameter ratios and the ratio of cross-sectional areas ($P < 0.001$), with an improved maintenance of root canal geometry by ProGlider and PathFile. At the coronal level and point of maximum canal curvature, ProGlider demonstrated a tendency to pre-flare the root canal compared with K-file and PathFile. PathFile and ProGlider demonstrated a significantly lower centroid shift compared with K-file at the apical level ($P = 0.023$). Post-shaping analysis demonstrated a more centred preparation of ProGlider, compared with PathFile and K-files, with no significant differences for other parameters.

Conclusions Use of ProGlider instruments led to less canal transportation than PathFiles and K-files.

Keywords: Glide path, Micro-CT, M-Wire, nickel–titanium, NiTi rotary instrumentation, ProGlider.

Received 12 January 2015; accepted 11 March 2016

Introduction

Use of nickel–titanium (NiTi) rotary instruments is associated with well-tapered root canal preparations, reduced operator fatigue and less time required for shaping, whilst also minimizing the risk of root canal transportation, compared with manual instrumentation (Gambill *et al.* 1996, Coleman & Svec 1997).

Correspondence: Dr. Damiano Pasqualini, Department of Surgical Sciences, CIR Dental School - Endodontics, University of Turin, via Nizza, 230, 10126 Torino, Italy (Tel.: +39(0) 11/6331569; e-mail: damiano.pasqualini@unito.it).

Improvements to shaping outcomes continue to simplify instrumentation protocols (Peters 2004, Hülsmann *et al.* 2005, Shen *et al.* 2013). However, instrument fracture, which is mainly dependent on bending and torsional stresses, remains a concern (Kuhn & Jordan 2002, Parashos & Messer 2006). Canal scouting and initial glide path with stainless steel sizes 08–10 K-files provide canal patency with tactile feedback and information regarding anatomy (Bürklein & Schäfer 2013). Subsequently, a glide path is prepared to create a smooth canal shape usually of a small taper (.02). Sizes 15 or 20 are recommended to prevent instrument blockage or taper lock (Roland *et al.* 2002, Blum *et al.* 2003, Berutti *et al.* 2004, 2009, Peters 2004), (American Association of Endodontists 2008). The intensity of torsional stresses affecting shaping instruments can therefore be reduced by creating manual or mechanical glide paths (Sattapan *et al.* 2000, Roland *et al.* 2002, Blum *et al.* 2003, Berutti *et al.* 2004, Patiño *et al.* 2005). Compared with manual glide path preparation, mechanical glide path preparation seems to be less technique-sensitive, resulting in an improved preservation of the canal anatomy, fewer canal aberrations, reduced time required for shaping and a lower incidence of postoperative pain (Berutti *et al.* 2009, 2012a, Lopes *et al.* 2012, Pasqualini *et al.* 2012a, Ajuz *et al.* 2013).

The ProGlider single-file system (Dentsply Maillefer, Ballaigues, Switzerland) is manufactured from M-Wire^{TM} alloy (Johnson *et al.* 2008) and consists of a single instrument with .02 taper and 0.16 mm diameter at its tip. The instrument is progressively tapered (up to .85) with an active part of 18 mm. ProGlider is recommended for use in continuous rotation (300 rpm; 2–5.2 Ncm torque) after canal patency has been verified with a size 10 K-file at working length (WL) (https://www.dentsply.com/content/dam/dentsply/pim/manufacturer/Endodontics/Glide_Path__Shaping/Rotary__Reciprocating_Files/Glide_Path/ProGlider_Rotary_Glide_Path_Files/ProGlider-DFU-kn8v8py-en-1409.pdf). The ProGlider instrument demonstrated greater flexibility and resistance to cyclic fatigue and torsional stresses, compared with the PathFile 2 (size 16, .02 taper, Dentsply Maillefer) (Elnaghy & Elsaka 2015). The progressive tapered design provides a glide path and preliminary enlargement of the root canal in the middle and coronal regions. This feature has been reported to reduce stress to the subsequent shaping NiTi rotary instrument (Berutti *et al.* 2014). However, little data exist on the capacity of this single-file glide path technique to maintain the original root canal anatomy. A previous study (Elnaghy & Elsaka 2014) reported better preservation of the original canal anatomy with ProGlider–ProTaper Next (Dentsply Maillefer) and PathFiles–ProTaper Next systems compared with ProTaper Next without glide path. The authors concluded that the fewer pecking motions required to complete shaping with ProTaper Next, especially when a glide path and initial flaring of the coronal and middle portion of the root canal previously achieved with the ProGlider instrument, could have led to reduced canal transportation. However, no information about the behaviour of the single-file ProGlider technique alone on canal geometry emerged from this study. Kirchhoff *et al.* (2015) evaluated apical transportation, canal volume increase and working time during glide path preparation with ProGlider and PathFile systems. ProGlider completed the glide path faster than PathFile; however, similar apical transportation and volume increases occurred in both groups. No data exist on the impact of glide path on post-shaping outcomes.

Several techniques have been used to evaluate shaping outcomes in *ex vivo* experimental models. X-ray computed micro-tomography (micro-CT) has emerged as a powerful tool for the evaluation of root canal morphology (Gambill *et al.* 1996, Peters 2004, Nair & Nair 2007, Paqué *et al.* 2009) as it enables the nondestructive analysis of key variables by matching high-resolution volume renderings of pre- and postoperative canal systems (Peters *et al.* 2003, Peters 2004, Loizides *et al.* 2007, Moore *et al.* 2009, Pasqualini *et al.* 2012b, Marceliano-Alves *et al.* 2015). Micro-CT findings have been reported to be comparable to those obtained by anatomical sectioning (Balto *et al.* 2000).

The primary objective of this micro-CT study was to evaluate the ability of ProGlider single file with augmented taper to preserve the original canal anatomy, compared with traditional 2% taper multiple file rotary PathFiles and manual (K-files) systems. The secondary objective was to analyse the impact of different glide path techniques on final root canal preparation with ProTaper Next. The null hypothesis was that there would be no differences between groups after glide path and shaping in severely curved root canals, with respect to canal volume and surface area, cross-sectional morphological parameters and centring ability.

Materials and methods

Specimen selection and preparation

Maxillary first permanent molars freshly extracted for periodontal disease were used in accordance with the local ethics committee. A sample size of 15 per group was calculated with G*Power 3.1.4 (Kiel University, Kiel, Germany) to set the study power at 80% (a large effect size equal to 1 was considered for the sample size computation). Specimens were immersed in a 0.01% NaOCl solution at 4 °C for 24 h following debridement of the root surface and then stored in saline solution.

A total of 64 teeth were selected. Specimens were mounted on a custom-made support, and low-resolution preliminary scans were performed to attain an overall outline of root canal anatomy and to ensure inclusion criteria were met.

Low-resolution preliminary scans were performed with the following parameters: a total of 450 projections through a 225° rotation (180° plus cone angle of the X-ray source) using a 1.0-mm-thick aluminium filter; voltage = 100 kV, current = 80 μA, source-to-object distance = 80 mm, source-to-detector distance = 220 mm, pixel binning = 8 × 8, exposure time/projection = 0.2 s. COBRA 7.2 (Exxim, Pleasanton, CA, USA) software was used to reconstruct the axial slices with an isotropic voxel size of 36 μm. Reconstructed axial slices in raw 16 bit format were equalized and converted to 8 bit TIFF file format with ImageJ 1.43u 64 bit software (National Institute of Health, Bethesda, MD, USA) and the reconstructed volumes were visualized using the VGStudio MAX 2.0 software (Volume Graphics GMBH, Heidelberg, Germany).

Morphological parameters of the mesio-buccal (MB1) canals were obtained. MB1 canals 12 ± 2 mm from canal orifice to apical foramen, 25–40° primary root curvature in clinical bucco-palatal view according to the Schneider method (Schneider 1971), $4 < r \leq 8$ mm main curvature radius (Gu *et al.* 2010) and a point of maximum curvature located within the middle third of the root canal were selected. The primary curvature was also investigated with a proximal view (after a 90° rotation of the specimen along its axis), and only teeth with a 10–30° primary curvature were included. Teeth with a distinct fourth canal orifice were utilized, so as to exclude teeth with a bucco-lingually flat mesio-buccal canal. Teeth with significant calcifications were excluded. Teeth not concurring with the aforementioned inclusion criteria regarding canal curvature and patency were excluded.

X-ray micro-CT analysis

The selected samples were then scanned at a higher spatial resolution, acquiring 2400 projections through a 360° rotation and using a 1.0-mm-thick aluminium filter. The following parameters were set for the high-resolution scans: voltage = 100 kV, current = 80 μA, source-to-object distance = 80 mm, source-to-detector distance = 220 mm, pixel binning = 2 × 2, exposure time/projection = 3 s (total scan duration = 2 h). COBRA 7.2 (Exxim) software was used to reconstruct the axial slices with an isotropic voxel size of 9.1 μm. Ring artifacts reduction was performed by the Pore3D software library developed at Elettra (Brun *et al.* 2010). Reconstructed axial slices in raw 16 bit format were equalized and converted to 8 bit TIFF file format with ImageJ 1.43u 64 bit software (National Institute of Health) with a whole stack volume of approximately 1200 × 1200 × 1200 voxels.

Image stacks were processed for volume registration and cutting plane selection by Amira 5.3.3 64 bit edition (Visage Imaging, Richmond, Australia). The registration algorithm was based on the mean square difference between the grey values of the two image sets. The alignment steps were set to 0.9 microns with a 0.0001 unit tolerance on the voxel intensity. Root canal paths were analysed with high-resolution 3D rendering and orthogonal cross sections to assess homogeneity of the groups at baseline (apical cross-sectional areas and diameters 1 mm from apical foramen, root canal surface area and volume). After checking the normality assumption (Shapiro–Wilk test), the degree of homogeneity was evaluated by one-way ANOVA (level of significance 5%).

Specimen preparation

Of 64 teeth assessed for inclusion, 19 were excluded due to anatomical features and severe calcification of the root canal. Forty-five teeth were randomly allocated to the experimental groups ($n = 15$): PathFile, ProGlider and hand K-files control group and between two experienced Clinical Assistant Professors in Endodontics with more than five years of experience using a computer-generated randomization table.

The operators were experienced in the techniques used and had been calibrated for pecking speed and pressure on the handpiece. New instruments were used for each specimen. Rotary instruments were used with in and out motion, with no intentional brushing effect. As each instrument required a specific technique, it was not possible to blind operators to their allocation. However, randomization, allocation and statistical analysis were all performed by blinded operators.

Following access cavity preparation, canal scouting and initial glide path were performed in all specimens with a size 10 K-file at WL using Glyde™ (Dentsply Maillefer, Ballaigues, Switzerland) as lubricating agent (0.80 mg) (Cruz *et al.* 2014). WL was established under 10× magnification (OPMI Pro Ergo, Carl Zeiss, Oberkochen, Germany) when the tip of the instrument was visible at the apical foramen and then subtracting 0.5 mm from this length.

The pulp chamber was filled with 5% NaOCl (Niclor 5, OGNA, Muggiò, Italy) throughout instrumentation, and 2 mL 5% NaOCl was used to irrigate the canal between each instrument for one minute.

Mechanical glide path preparation in the PathFile test group (n = 15) was performed with NiTi rotary PathFile 1 and 2 (tip sizes 0.13 and 0.16 mm, respectively, taper .02) (Dentsply Maillefer) and an endodontic motor (X-Smart, Dentsply Maillefer) with 16 : 1 contra angle at 300 rpm, 5 Ncm at full WL.

Mechanical glide path in the ProGlider test group (n = 15) was performed with NiTi rotary ProGlider single file (tip size 0.16 mm, taper .02) (Dentsply Maillefer) and an endodontic engine with 16 : 1 contra angle, at 300 rpm, 5 Ncm at full WL.

Manual glide path in the K-file control group (n = 15) was carried out with stainless steel sizes 12 to 15 K-FlexoFiles (Dentsply Maillefer), used with a 'feed in and pull' motion (watch-winding motion and then moved coronally after engagement)until full WL. All specimens were then shaped with ProTaper Next X1 (0.17, .04 to .075 taper) and X2 (0.25, .06 to .07 taper) (Dentsply Maillefer) using the X-Smart motor (300 rpm, 4 Ncm) at WL. Instruments were removed from the canal and cleaned each time after three pecking motions until WL was reached.

The number of pecking motions and the time (s) required for glide path and shaping with ProTaper Next X1 and X2 were recorded.

Irrigation was carried out with disposable conventional hand-held syringes and 30G needles taken 2 mm short of the WL without engaging root canal walls. Alternating 5% NaOCl with 10% EDTA was used to provide a total of 10 mL of each irrigant solution per specimen. Recapitulation with a size 10 K-file was performed between each instrument. Root canals were dried with absorbent sterile paper points and micro-scanned for post-treatment analyses.

Micro-CT 3D and 2D imaging analysis

Three-dimensional models of the root canals, before preparation, after glide path preparation and after shaping with ProTaper Next, were matched and micro-CT scans were managed as previously described to enable pre- and postoperative evaluation for each group. Three-dimensional (volume and surface area) and 2D (root canal gravity centre, ratio of diameter ratios and ratio of cross-sectional areas) parameters were assessed. Root canal volumes were calculated as the volume of binarized objects within the volume of interest. Surface areas were extracted by the vertical surfaces exposed by pixel differences between adjacent cross sections (Versiani *et al.* 2013). Increases in volume and surface areas were analysed for each group by subtracting the scores for the untreated canals from those recorded for their treated counterparts.

Root canal sections orthogonal to the canal axis were set at three levels: apical (A), 1 mm from the apical foramen; middle (M), set at the point of maximum curvature; and coronal (C), set in correspondence to the middle portion of the root canal coronal third defined by 3D calculation of the root canal length from apex to orifice. These were selected as areas most representative of the critical shaping points (Jafarzadeh & Abbott 2008), and 2D parameters were analysed at each level. The same cutting plane orientation was used for pre- and post-treatment samples. Axial slices were imported in TIFF format and analysed with ImageJ using a minimum threshold algorithm (MT). The MT was implemented in the auto threshold item built within the Image menu (ImageJ) to avoid manual errors (Neves *et al.* 2015). Micro-CT analyses were performed preoperatively and both after glide path and shaping and data were collected by an experienced operator who was blind to specimen allocation.

The major diameter was calculated as the distance between the two most distant pixels in the object. The minor diameter was defined as the longest chord orthogonal to the respective major diameter (Versiani *et al.* 2013). Canal transportation was assessed from centres of gravity that were calculated for each slice

(Peters *et al.* 2000, Peters & Paqué 2011). The centre of gravity for each scanning slice at the three levels of analysis (A, M and C) was traced, and coordinates on both axes of planar images were recorded. The average of the x- and y-coordinates of all pixels in the selection was automatically traced using ImageJ software through the 'centroid' algorithm, following the automated 'wand tracing' tool of the threshold root canal space. Average canal transportation was subsequently calculated by the centroid shift, in millimetres, before and after instrumentation.

Ratio of diameter ratios (RDR) and ratio of cross-sectional areas (RA) indicators were used to evaluate canal geometry modifications induced by preparation, as previously published (Pasqualini *et al.* 2012b).

1. RDR represents the instrument tendency to asymmetrically enlarge the root canal in one direction: that is RDR = $(D/d)_{post}/(D/d)_{pre}$, where $(D/d)_{post}$ is the post-preparation ratio of the major diameter (D) to the minor diameter (d) and $(D/d)_{pre}$ is the pre-preparation ratio of D to d. Score 1 corresponds to no difference in ratios between post- and pre-instrumentation measurements. Values closer to 1 correspond to a better maintenance of the original canal geometry, whilst deviation from 1 corresponds to a less symmetrical preparation compared to the original anatomy.
2. RA quantifies the ability of the instrument to enlarge the root canal space: that is RA = A_{post}/A_{pre}, where A_{post} and A_{pre} are the post-preparation and the pre-preparation cross-sectional areas, respectively. Values closer to 1 correspond to a reduced difference between post- and pre-instrumentation measurements. Assuming similar baseline characteristics of the root canals, values closer to 1 correspond to a reduced enlargement.

Statistical analysis

Data distribution was analysed with the Shapiro–Wilk normality test. Differences in canal curvature at baseline and shift of canal centre of gravity at the M level were analysed by the Kruskall–Wallis test and *post hoc* Dunn's test ($P < 0.05$). One-way ANOVA and *post hoc* Tukey–Kramer test ($P < 0.05$) were used to analyse differences in the increase in surface area and canal volume and shift in canal centre of gravity at the A and C level.

One-way ANOVAs were performed to evaluate the impact of instrumentation (K-file/PathFile/ProGlider) on RDR and RA at each level of analysis (A, M and C). Tukey–Kramer test was utilized as a *post hoc* test. The significance level was set to 5% ($P < 0.05$). All statistical analyses were performed using the Minitab 15 software package (Minitab Inc., State College, PA, USA).

Results

The mean curvature of specimens was 33.1° ± 3.8° (min = 26°, max = 40°), 34.4° ± 4.1° (min = 28°, max = 39°) and 34.9° ± 3.8° (min = 27°, max = 40°) in the K-file, PathFile and ProGlider groups, respectively, with no differences between groups ($P = 0.14$). There was no incidence of instrument fracture during canal preparation. Canal volumes, surface areas and mean apical diameters at baseline are presented in Table 1. The values displayed preoperative homogeneity between groups.

Figures 1 and 2 represent, respectively, 3D and 2D matching of preoperative (green), post-glide path (red) and post-shaping (blue) canal volume and sections at the apical (A), middle third at point of maximum curvature (M) and coronal (C) levels of analysis in all groups.

The increase in canal volumes and surface areas, shift of canal centres of gravity and RDR and RA after glide path and shaping are presented in Tables 2 and 3.

Post-glide path results

The mean number of pecking motions to complete the glide path was 7.2 ± 1.17 in the PathFile group and 3.80 ± 1.75 in the ProGlider group; the mean

Table 1 Sample baseline characteristics in all groups (mean, STD)

	KF	PF	PG	P
Canal volumes (mm^3)	2.08 ± 0.83	2.27 ± 0.79	2.09 ± 0.90	0.15
Canal surface area (mm^2)	15.97 ± 4.70	16.22 ± 3.78	16.61 ± 3.73	0.77
Apical diameters[a] (mm)	0.17 ± 0.06	0.18 ± 0.04	0.16 ± 0.05	0.45

KF, hand K-file; PF, PathFile; PG, ProGlider.
Statistical significance indicated by $P < 0.05$
[a]Apical diameters (mean±SD) at 1 mm from apical foramen

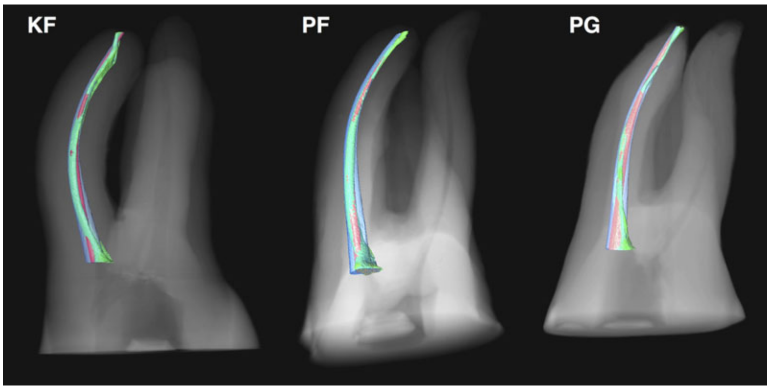

Figure 1 Representative images of matching 3D reconstructions pre-treatment (green), post-glide path (red) and post-shaping with ProTaper Next X1 and X2 (blue); hand K-files; ProGlider; PathFile groups.

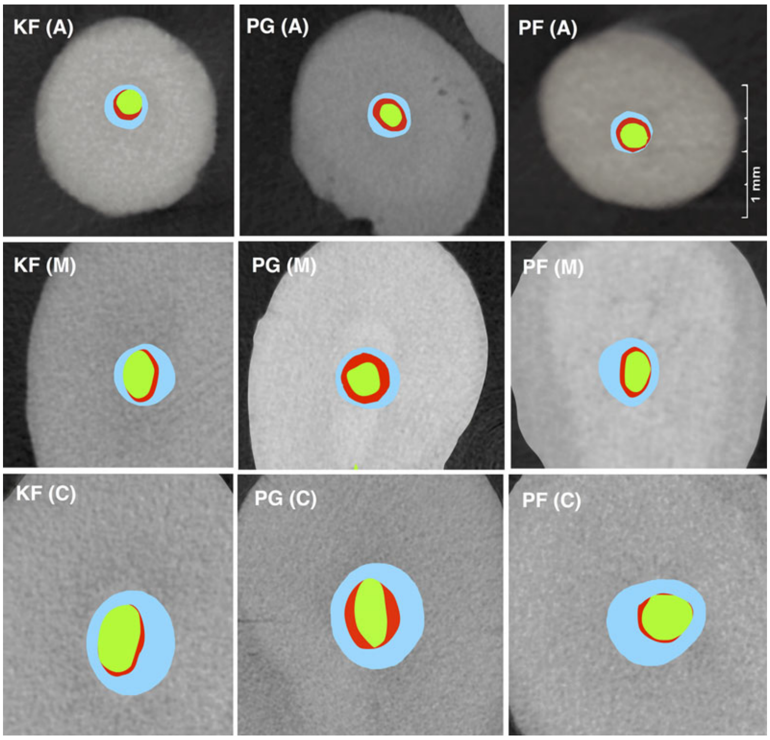

Figure 2 Image matching of pre-instrumentation, post-glide path and post-shaping sections, according to the previously selected cutting plane. Note the difference between pre-treatment (green) post-glide path (red) and post-shaping with ProTaper Next X1 and X2 (blue) specimens at the apical (A), middle third at maximum curvature (M) and coronal (C) levels of analysis. Hand K-files; ProGlider; PathFile groups.

instrumentation time (s) was 14.25 ± 1.37 in the PathFile group and 6.8 ± 0.84 in the ProGlider group. There was a significant difference between the groups ($P = 0.0001$) for both parameters.

ProGlider instrumentation enlarged the root canal space with a significant increase in canal volume ($P < 0.0001$) and surface area ($P = 0.0009$) compared with K-file and PathFile groups.

Hand K-files demonstrated a significant increase in centre of gravity shift compared with NiTi rotary PathFile and ProGlider at the A point of analysis ($P = 0.023$). No differences emerged from *post hoc*

Table 2 3D and 2D parameters utilized for post-instrumentation analysis in each group (KF = hand K-file; PF = PathFile; PG = ProGlider)

	Increase in canal volume (mm^3)		Increase in canal surface area (mm^2)			Centre of gravity shift (mm^{-1})		RDR		RA	
Group	Range	Mean±SD	Range	Mean±SD	Level of analysis	Range	Mean±SD	Range	Mean±SD	Range	Mean±SD
KF	0.05–0.37	0.20 ± 0.09^{a}	0.48–0.9	0.67 ± 0.1^{a}	Coronal	0.09–0.61	0.27 ± 0.21^{a}	0.95–1.04	0.99 ± 0.04^{a}	0.97–1.10	1.05 ± 0.04^{a}
					Middle	0.05–1.60	0.52 ± 0.41^{a}	0.96–1.15	1.10 ± 0.07^{a}	1.02–1.46	1.18 ± 0.15^{a}
					Apical	0.33–0.82	0.55 ± 0.16^{a}	0.77–1.18	0.90 ± 0.05^{b}	1.02–1.42	1.32 ± 0.12^{a}
PF	0.09–0.41	0.22 ± 0.08^{a}	0.25–1.06	0.65 ± 0.21^{a}	Coronal	0.04–0.63	0.20 ± 0.16^{a}	0.66–1.23	1.08 ± 0.08^{a}	1.01–1.20	1.07 ± 0.06^{a}
					Middle	0.09–0.48	0.36 ± 0.20^{a}	0.71–1.25	1.02 ± 0.15^{a}	1.02–1.76	1.12 ± 0.21^{a}
					Apical	0.03–0.82	0.36 ± 0.25^{b}	0.87–1.28	1.03 ± 0.11^{a}	1.03–1.31	1.20 ± 0.38^{a}
PG	0.14–0.67	0.39 ± 0.15^{b}			Coronal	0.03–0.90	0.34 ± 0.26^{a}	0.58–1.13	0.94 ± 0.17^{a}	1.06–1.56	1.14 ± 0.16^{b}
			0.46–1.15	0.90 ± 0.2^{b}	Middle	0.12–1.10	0.39 ± 0.30^{a}	0.82–1.21	0.98 ± 0.09^{a}	0.98–1.52	1.31 ± 0.07^{b}
					Apical	0.25–0.70	0.37 ± 0.13^{b}	0.87–1.17	0.99 ± 0.14^{a}	1.03–1.38	1.15 ± 0.94^{a}

Different superscript letters in the same column indicate significant differences between groups ($P < 0.05$). For 2D parameters (centre of gravity shift, RDR and RA), significance was compared for the same level of analysis (coronal, middle or apical).

Table 3 3D and 2D parameters utilized for post-shaping analysis in each group (KF = hand K-file; PF = PathFile; PG = ProGlider)

	Increase in canal volume (mm^3)		Increase in canal surface area (mm^2)			Centre of gravity shift (mm^{-1})		RDR		RA	
Group	Range	Mean±SD	Range	Mean±SD	Level of analysis	Range	Mean±SD	Range	Mean±SD	Range	Mean±SD
KF	0.24–1.77	0.97 ± 0.48^{a}	1.05–5.15	2.74 ± 1.13^{a}	Coronal	0.9–1.9	1.54 ± 0.30^{a}	0.32–1.21	0.84 ± 0.26^{a}	2.16–3.72	2.84 ± 0.47^{a}
					Middle	0.5–1.8	1.24 ± 0.48^{a}	0.49–1.32	0.76 ± 0.24^{a}	1.12–2.91	2.16 ± 0.54^{a}
					Apical	0.2–1.9	1.32 ± 0.44^{a}	0.53–1.43	0.91 ± 0.25^{a}	1.37–1.94	1.61 ± 0.17^{a}
PF	0.56–1.45	0.94 ± 0.25^{a}	0.91–5.23	2.72 ± 1.14^{a}	Coronal	0.7–1.8	1.34 ± 0.41^{a}	0.38–1.18	0.82 ± 0.26^{a}	2.28–3.13	2.64 ± 0.27^{a}
					Middle	0.6–1.6	1.15 ± 0.27^{a}	0.56–1.15	0.81 ± 0.19^{a}	1.10–2.86	1.99 ± 0.59^{a}
					Apical	0.7–1.7	1.02 ± 0.28^{a}	0.42–1.32	0.86 ± 0.25^{a}	1.47–1.92	1.70 ± 0.14^{a}
PG	0.24–1.71	0.87 ± 0.50^{a}	0.84–6.88	2.77 ± 2.04^{a}	Coronal	0.2–1.3	0.61 ± 0.36^{b}	0.45–1.34	0.85 ± 0.27^{a}	1.52–3.72	2.80 ± 0.5^{a}
					Middle	0.4–1.3	0.73 ± 0.26^{b}	0.59–1.31	0.95 ± 0.24^{a}	1.06–2.84	1.93 ± 0.62^{a}
					Apical	0.1–1.2	0.45 ± 0.29^{b}	0.68–1.23	0.90 ± 0.17^{a}	1.16–2.66	1.61 ± 0.34^{a}

Different superscript letters in the same column indicate significant differences between groups ($P < 0.05$). For 2D parameters (centre of gravity shift, RDR and RA), significance was compared for the same level of analysis (coronal, middle or apical).

analysis between PathFile and ProGlider. No differences were found between groups in centring ability at C and M points of analysis.

RDR and RA were closer to 1 in the ProGlider and PathFile groups at A, indicating that canal geometry modifications were significantly reduced compared with hand instrumentation, where asymmetrical increases in canal diameters and cross-sectional area occurred. RDR was closer to 1 in the ProGlider and PathFile groups at M, indicating that canal modifications were reduced compared with hand instrumentation. However, the differences were not significant. RA was further from 1 in the ProGlider group at M and C compared with the PathFile and K-File groups, demonstrating a tendency of ProGlider to produce a more evident enlargement of the root canal in the middle and coronal portions of the canals.

Canal shaping results

The mean number of pecking motions with ProTaper Next X1 and X2 was 15.8 ± 2.32 in the PathFile group, 11.6 ± 1.36 in the ProGlider group and 16.2 ± 2.81 in the K-file group. The difference between groups was significant ($P = 0.02$). The mean instrumentation time (s) was 26.8 ± 2.85 in the PathFile group, 23.95 ± 4.14 in the ProGlider group and 27.7 ± 3.01 in K-file group, with no significant difference ($P = 0.08$) between the groups.

The ProGlider group had a significantly reduced centre of gravity shift compared with PathFile and K-file groups at A, M and C points of analysis ($P < 0.05$). No significant differences emerged between groups for other 3D and 2D parameters (Table 3).

Discussion

Initial canal scouting and glide path preparation are the first instrumentation steps of root canal procedures, and these are associated with high rates of procedural errors and ledge formation (Jafarzadeh & Abbott 2008). Despite the benefits of mechanical glide path (Berutti *et al.* 2009, Pasqualini *et al.* 2012a,b), contrasting studies have not demonstrated any differences between manual or rotary glide path (Alves Vde *et al.* 2012) and both techniques are considered clinically reliable (Bürklein & Schäfer 2013). Therefore, manual glide path with stainless steel K-files is still considered a valid technique when compared with new NiTi rotary glide path systems (Alves Vde *et al.* 2012) (Bürklein & Schäfer 2013).

Micro-CT scanning is a valuable and reproducible method for evaluating root canals prepared with NiTi rotary instruments or stainless steel endodontic files (Peters *et al.* 2001, 2003, Loizides *et al.* 2007, Nair & Nair 2007, Moore *et al.* 2009, Paqué *et al.* 2009, Pasqualini *et al.* 2012b, Zhao *et al.* 2013). Matching volume rendering of teeth obtained with X-ray micro-CT before and after treatment enables the 3D analysis of canal volume and surface area (Peters *et al.* 2003, Capar *et al.* 2014) and 2D analysis of root canal sections orthogonal to the canal axis at different levels (Peters 2004, Nair & Nair 2007, Pasqualini *et al.* 2012b). In this study, ProGlider significantly increased canal volume and surface area compared with manual and mechanical glide path with PathFiles, probably due to its progressive taper design. The present findings are in contrast to a previous study (Kirchhoff *et al.* 2015), which reported similar volume increases during glide path management with PathFiles and ProGliders. However, the ProGlider system (size 16, .02 taper at the tip) was compared with the PathFile system until size 3 (size 19, .02 taper). In the present study, NiTi rotary glide path instruments (PathFile and ProGlider) demonstrated significantly better maintenance of the original canal anatomy compared with hand K-files, with less impact on the canal axis (Zhao *et al.* 2013) and root canal geometry, especially in the apical region. Baseline homogeneity was assumed between groups for cross-sectional area and diameter at point A. Results were compatible with instrument effectiveness against canal walls and displayed coherence with data from the literature (Table 1) (Marroquín *et al.* 2004). Furthermore, RDR and RA analyses indicated that hand K-files impacted on the original canal geometry at the apical level with a less symmetrical enlargement of the root canal in each direction. Regarding apical transportation, findings are in agreement with previous studies (Kirchhoff *et al.* 2015). NiTi rotary instruments used to create glide paths should ideally be small and flexible to permit safe and efficient progression in an apical direction (Ajuz *et al.* 2013, Haapasalo & Shen 2013, Nakagawa *et al.* 2014). Previous micro-CT analysis confirmed the ability of NiTi rotary PathFiles to perform glide paths and better preserve the original root canal geometry (Pasqualini *et al.* 2012b, Ajuz *et al.* 2013), and they were selected as the NiTi rotary control group. Alternatively, stainless steel K-files, due to their increased stiffness, have a higher tendency to straighten the canal and to create aberrations such as apical zips and elbows (Pettiette *et al.* 1999, Berutti *et al.* 2009).

The ProGlider instrument is recommended for use prior to ProTaper Next X1 with tip size 17, immediately following size 10 K-file to passively reach full WL, verifying canal patency. However, its tip size 0.16 mm is considered sufficient for minimizing taper lock for nearly all first instruments of similar tip size used in shaping systems (Elnaghy & Elsaka 2015).

ProGlider instruments demonstrated a tendency to create a preliminary enlargement of the root canal in the coronal and middle portions due to its progressive tapered design. Preliminary enlargement of the root canal allows WL files to more consistently reach the apical foramen, significantly increasing the precision of electronic apex locators to determine the real WL (Ibarrola *et al.* 1999). Moreover, a laboratory study demonstrated that preliminary enlargement of the root canal, with elimination of middle and coronal interferences with ProGlider, reduced the amount of stress stored by ProTaper Next X1 during shaping (Berutti *et al.* 2014). A previous study (Elnaghy & Elsaka 2014) reported that glide path preparation with ProGlider could reduce canal transportation after shaping with ProTaper Next X2. However, it was not clear whether the findings were influenced by the superior centring ability of ProGlider or only by reduced stress and number of pecking motions required to complete shaping with ProTaper Next. The primary objective of this study was to investigate whether glide path creation could be effectively performed by a NiTi rotary single file of augmented taper and to compare this technique with existing 2% taper multiple file NiTi rotary and manual techniques.

However, subsequent rotary instrumentation may eliminate such differences amongst the tested groups, thus rendering clinical relevance debatable. Therefore, the effects of ProTaper Next shaping on 3D and 2D geometric parameters in the three different groups were assessed.

In the present study, all final instruments had a similar tip size to ensure comparability of micro-CT outcomes and an homogeneous baseline for the subsequent shaping phase. Two different operators previously calibrated were involved in the study to increase the external validity of the results obtained (Bergenholtz & Kvist 2014) and to optimize timing of the instrumentation phase with a reduction in the storage time for specimens. Chelating agent in gel was utilized during canal scouting and initial glide path, and 10% EDTA liquid solution alternated with 5% NaOCl was used as irrigant during completion of the glide path and shaping. Regardless of whether liquid chelating agents more effectively remove smear layer (Hülsmann *et al.* 2002, Lim *et al.* 2003, Cruz *et al.* 2014), previous studies suggest that the use of liquid or gel-like chelating agents during instrumentation may not significantly affect root canal transportation (Whitbeck *et al.* 2015).

Canal volume and surface area variation were not different amongst groups after shaping with ProTaper Next X2, thus supporting the hypothesis that different glide path systems did not affect final preparation with respect to these parameters.

However, according to previous study (Elnaghy & Elsaka 2014), ProGlider seemed to improve ProTaper Next performance by positively influencing geometrical shaping outcomes. In the ProGlider group, the centre of gravity shift after shaping with ProTaper Next at the three levels of analysis was lower than PathFile and K-file. As significant differences were reported in number of pecking motions during shaping with ProTaper Next in the ProGlider group, results might be attributed to this aspect beside the satisfactory centring ability of ProGlider. Therefore, a glide path preserving the original canal anatomy, with fewer canal aberrations and the lowest variation in canal geometry and centring, particularly at the apical level, may provide more favourable conditions for the subsequent shaping phase.

Conclusions

The ProGlider single NiTi rotary instrument appears suitable for glide path management as it was associated with less canal transportation after shaping procedures with ProTaper Next X1 and X2.

Acknowledgements

The authors gratefully thank Dr. Elisa Bottero and Dr. Andrea Roggia (Lecturers at University of Turin Dental School) for kind and valuable support. D. Pasqualini declares lecturing personal fees for Dentsply Maillefer in the last 3 years. The other authors declare no competing conflict of interests with the materials discussed in this manuscript. MicroCT scanning were performed at TomoLab X-ray micro-CT laboratory at Elettra – Sincrotrone Trieste S.C.p.A., http://www.elettra.trieste.it/light-sources/labs-and-services/tomolab/tomolab.html.

Conflict of interests

Dr Pasqualini reports personal fees from Dentsply Maillefer, outside the submitted work. The other authors have stated explicitly that there is no conflict of interests in connection with this article.

References

Ajuz NC, Armada L, Gonçalves LS, Debelian G, Siqueira JF Jr (2013) Glide path preparation in S-shaped canals with rotary pathfinding nickel-titanium instruments. *Journal of Endodontics* **39**, 534–7.

Alves Vde O, Bueno CE, Cunha RS, Pinheiro SL, Fontana CE, de Martin AS (2012) Comparison among manual instruments and PathFile and Mtwo rotary instruments to create a glide path in the root canal preparation of curved canals. *Journal of Endodontics* **38**, 117–20.

American Association of Endodontists (2008) Colleagues for Excellence. Rotary Instrumentation: an Endodontic Perspective. URL http://www.aae.org/uploadedfiles/publications_and_research/endodontics_colleagues_for_excellence_newsletter/winter08ecfe.pdf.

Balto K, Müller R, Carrington DC, Dobeck J, Stashenko P (2000) Quantification of periapical bone destruction in mice by micro-computed tomography. *Journal of Dental Research* **79**, 35–40.

Bergenholtz G, Kvist T (2014) Evidence-based endodontics. *Endodontic Topics* **31**, 3–18.

Berutti E, Negro AR, Lendini M, Pasqualini D (2004) Influence of manual preflaring and torque on the failure rate of ProTaper rotary instruments. *Journal of Endodontics* **30**, 228–30.

Berutti E, Cantatore G, Castellucci A *et al.* (2009) Use of nickel-titanium rotary PathFile to create the glide path: comparison with manual preflaring in simulated root canals. *Journal of Endodontics* **35**, 408–12.

Berutti E, Paolino DS, Chiandussi G *et al.* (2012a) Root canal anatomy preservation of WaveOne reciprocating files with or without glide path. *Journal of Endodontics* **38**, 101–4.

Berutti E, Alovisi M, Pastorelli MA, Chiandussi G, Scotti N, Pasqualini D (2014) Energy consumption of ProTaper Next X1 after Glide Path with PathFiles and ProGlider. *Journal of Endodontics* **40**, 2015–8.

Blum JY, Machtou P, Ruddle C, Micallef JP (2003) Analysis of mechanical preparations in extracted teeth using ProTaper rotary instruments: value of the safety quotient. *Journal of Endodontics* **29**, 567–75.

Brun F, Mancini L, Kasae P, Favretto S, Dreossi D, Tromba G (2010) Pore3D: a software library for quantitative analysis of porous media. *Nuclear Instruments and Methods in Physics Research Section A* **615**, 326–32.

Bürklein S, Schäfer E (2013) Critical evaluation of root canal transportation by instrumentation. *Endodontic Topics* **29**, 110–24.

Capar ID, Ertas H, Ok E, Arslan H, Ertas ET (2014) Comparative study of different novel nickel-titanium rotary systems for root canal preparation in severely curved root canals. *Journal of Endodontics* **40**, 852–6.

Coleman CL, Svec TA (1997) Analysis of Ni-Ti versus stainless steel instrumentation in resin simulated canals. *Journal of Endodontics* **23**, 232–5.

Cruz A, Vera J, Gascón G, Palafox-Sánchez CA, Amezcua O, Mercado G (2014) Debris remaining in the apical third of root canals after chemomechanical preparation by using sodium hypochlorite and glyde: an invivo study. *Journal of Endodontics* **40**, 1419–23.

Elnaghy AM, Elsaka SE (2014) Evaluation of root canal transportation, centering ratio, and remaining dentin thickness associated with ProTaper Next instruments with and without glide path. *Journal of Endodontics* **40**, 2053–6.

Elnaghy AM, Elsaka SE (2015) Evaluation of the mechanical behaviour of PathFile and ProGlider pathfinding nickel-titanium rotary instruments. *International Endodontic Journal* **48**, 894–901.

Gambill JM, Alder M, del Rio CE (1996) Comparison of nickel-titanium and stainless steel hand-file instrumentation using computed tomography. *Journal of Endodontics* **22**, 369–75.

Gu Y, Lu Q, Wang P, Ni L (2010) Root canal morphology of permanent three-rooted mandibular first molars: part II–measurement of root canal curvatures. *Journal of Endodontics* **36**, 1341–6.

Haapasalo M, Shen Y (2013) Evolution of nickel–titanium instruments: from past to future. *Endodontic Topics* **29**, 3–17.

Hülsmann M, Heckendorff M, Schäfers F (2002) Comparative in-vitro evaluation of three chelator pastes. *International Endodontic Journal* **35**, 668–79.

Hülsmann M, Peters OA, Dummer P (2005) Mechanical preparation of root canals: shaping goals, techniques and means. *Endodontic Topics* **10**, 30–76.

Ibarrola JL, Chapman BL, Howard JH, Knowles KI, Ludlow MO (1999) Effect of preflaring on Root ZX apex locators. *Journal of Endodontics* **25**, 625–6.

Jafarzadeh H, Abbott PV (2008) Ledge formation: review of a great challenge in endodontics. *Journal of Endodontics* **33**, 1155–62.

Johnson E, Lloyd A, Kuttler S, Namerow K (2008) Comparison between a novel nickel-titanium alloy and 508 nitinol on the cyclic fatigue life of ProFile 25/.04 rotary instruments. *Journal of Endodontics* **34**, 1406–9.

Kirchhoff AL, Chu R, Mello I, Garzon AD, Dos Santos M, Cunha RS (2015) Glide Path management with single- and multiple-instrument rotary systems in curved canals: a micro-computed tomographic study. *Journal of Endodontics* **41**, 1880–3.

Kuhn G, Jordan L (2002) Fatigue and mechanical properties of nickel-titanium endodontic instruments. *Journal of Endodontics* **28**, 716–20.

Lim TS, Wee TY, Choi MY, Koh WC, Sae-Lim V (2003) Light and scanning electron microscopic evaluation of GlydeTM

File Prep in smear layer removal. *International Endodontic Journal* **36**, 336–43.

Loizides AL, Kakavetsos VD, Tzanetakis GN, Kontakiotis EG, Eliades G (2007) A comparative study of the effects of two nickel-titanium preparation techniques on root canal geometry assessed by microcomputed tomography. *Journal of Endodontics* **33**, 1455–9.

Lopes HP, Elias CN, Siqueira JF Jr *et al.* (2012) Mechanical behavior of pathfinding endodontic instruments. *Journal of Endodontics* **38**, 1417–21.

Marceliano-Alves MF, Sousa-Neto MD, Fidel SR *et al.* (2015) Shaping ability of single-file reciprocating and heat-treated multifile rotary systems: a micro-CT study. *International Endodontic Journal* **48**, 1129–36.

Marroquín BB, El-Sayed MA, Willershausen-Zönnchen B (2004) Morphology of the physiological foramen: I. Maxillary and mandibular molars. *Journal of Endodontics* **30**, 321–8.

Moore J, Fitz-Walter P, Parashos P (2009) A micro-computed tomographic evaluation of apical root canal preparation using three instrumentation techniques. *International Endodontic Journal* **42**, 1057–64.

Nair MK, Nair UP (2007) Digital and advanced imaging in endodontics: a review. *Journal of Endodontics* **33**, 1–6.

Nakagawa RK, Alves JL, Buono VT, Bahia MG (2014) Flexibility and torsional behaviour of rotary nickel-titanium PathFile, RaCe ISO 10, Scout RaCe and stainless steel K-File hand instruments. *International Endodontic Journal* **47**, 290–7.

Neves AA, Silva EJ, Roter JM *et al.* (2015) Exploiting the potential of free software to evaluate root canal biomechanical preparation outcomes through micro-CT images. *International Endodontic Journal* **48**, 1033–42.

Paqué F, Ganahl D, Peters OA (2009) Effects of root canal preparation on apical geometry assessed by micro-computed tomography. *Journal of Endodontics* **35**, 1056–9.

Parashos P, Messer HH (2006) Rotary NiTi instrument fracture and its consequences. *Journal of Endodontics* **32**, 1031–43.

Pasqualini D, Mollo L, Scotti N *et al.* (2012a) Postoperative pain after manual and mechanical glide path: a randomized clinical trial. *Journal of Endodontics* **38**, 32–6.

Pasqualini D, Bianchi CC, Paolino DS *et al.* (2012b) Computed micro-tomographic evaluation of glide path with nickel-titanium rotary PathFile in maxillary first molars curved canals. *Journal of Endodontics* **38**, 389–93.

Patiño PV, Biedma BM, Liébana CR, Cantatore G, Bahillo JG (2005) The influence of a manual glide path on the separation rate of NiTi rotary instruments. *Journal of Endodontics* **31**, 114–6.

Peters OA (2004) Current challenges and concepts in the preparation of root canal systems: a review. *Journal of Endodontics* **30**, 559–67.

Peters OA, Paqué F (2011) Root canal preparation of maxillary molars with the self-adjusting file: a micro-computed tomography study. *Journal of Endodontics* **37**, 53–7.

Peters OA, Laib A, Rüegsegger P, Barbakow F (2000) Three-dimensional analysis of root canal geometry using high-resolution computed tomography. *Journal of Dental Research* **79**, 1405–9.

Peters OA, Laib A, Göhring TN, Barbakow F (2001) Changes in root canal geometry after preparation assessed by high-resolution computed tomography. *Journal of Endodontics* **27**, 1–6.

Peters OA, Peters CI, Schönenberger K, Barbakow F (2003) ProTaper rotary root canal preparation: effects of canal anatomy on final shape analysed by micro CT. *International Endodontic Journal* **36**, 86–92.

Pettiette MT, Metzger Z, Phillips C, Trope M (1999) Endodontic complications of root canal therapy performed by dental students with stainless-steel K-files and nickel-titanium hand files. *Journal of Endodontics* **25**, 230–4.

Roland DD, Andelin WE, Browning DF, Hsu GH, Torabinejad M (2002) The effect of preflaring on the rates of separation for 0.04 taper nickel titanium rotary instruments. *Journal of Endodontics* **28**, 543–5.

Sattapan B, Nervo GJ, Palamara JE, Messer HH (2000) Defects in rotary nickel-titanium files after clinical use. *Journal of Endodontics* **26**, 161–5.

Schneider SW (1971) A comparison of canal preparations in straight and curved root canals. *Oral Surgery, Oral Medicine, and Oral Pathology* **32**, 271–5.

Shen Y, Zhou HM, Zheng YF, Peng B, Haapasalo M (2013) Current challenges and concepts of the thermomechanical treatment of nickel-titanium instruments. *Journal of Endodontics* **39**, 163–72.

Versiani MA, Pécora JD, Sousa-Neto MD (2013) Microcomputed tomography analysis of the root canal morphology of single-rooted mandibular canines. *International Endodontic Journal* **46**, 800–7.

Whitbeck ER, Swenson K, Tordik PA, Kondor SA, Webb TD, Sun J (2015) Effect of EDTA preparations on rotary root canal instrumentation. *Journal of Endodontics* **41**, 92–6.

Zhao D, Shen Y, Peng B, Haapasalo M (2013) Micro-computed tomography evaluation of the preparation of mesiobuccal root canals in maxillary first molars with Hyflex CM, Twisted Files, and K3 instruments. *Journal of Endodontics* **39**, 385–8.